Energy 133 (2017) 191–205

Contents lists available at ScienceDirect

Energy

journal homepage: www.elsevier.com/locate/energy

A techno-economic assessment of offshore wind energy in Chile

Cristian Mattar*, María Cristina Guzmán-Ibarra

Laboratory for Analysis of the Biosphere (LAB), University of Chile, Chile

ARTICLE INFO

Article history:
Received 14 October 2016
Received in revised form
11 May 2017
Accepted 15 May 2017
Available online 19 May 2017

Keywords:
Offshore wind power
ERA interim
LCOE
Chile

ABSTRACT

Offshore wind energy potential and its technical and economic feasibility were determined in Chile. Wind speed data from ERA-Interim reanalysis 10 m above the sea surface between 1979 and 2014 was used. The capacity factor and performance of the V164–8.0 MW wind generator was also determined. Using this information along with data from other studies, the following economic indicators were calculated: Levelized Cost Of Energy (LCOE), Net Present Value (NPV), Internal Rate of Return (IRR) and Pay-Back (PB). The results show that the area between 45 and 56°S has the highest values in terms of both power density (~3190 W/m^2) and capacity factor (~70%), as well as the lowest LCOE values (72–100 USD $/MWh). The area between 30 and 32°S was estimated to be the most suitable area for implementing an offshore wind project because of its wind power density (between 700 W/m2 and 900 W/m2), capacity factors between 40% and 60%, LCOE between 100 and 114 USD$/MWh. This work shows how important studying Chile's offshore wind power is for to be used and for removing barriers to current knowledge about this renewable energy and the benefits it would bring to Chile's power array.
© 2017 Elsevier Ltd. All rights reserved.

1. Introduction

In recent decades, wind energy has seen improvements in efficiency and reducing unit costs of wind turbines, thus making it a competitive alternative to other energy sources [40,44]. In fact, installed wind power capacity has been growing rapidly worldwide where it has been supplemented by policy-making that incentivizes its use, crucial to its development in different countries [22]. Based on the latest report from the *Global Wind Energy Council* (GWEC) [17], installed wind power capacity reached ~ 370 GW by the end of 2015, a cumulative market growth of 16%. In light of this, its large-scale use is expected to increase in the decades to come [14].

One of the main characteristics of offshore wind farms is their high energy density [40], which might even be comparable to conventional power plants in terms of their production capacity [42]. This is because sea surface wind experiences fewer disturbances as there are rarely any obstacles producing turbulence, and therefore better use of the wind for power generation [21]. Locating wind farms offshore is also an alternative when facing constraints on land availability and issues arising due to the noise and visual pollution caused by onshore wind farms [54]. However, offshore wind farms end up being more expensive to install and maintain than onshore facilities, where the levelized cost is estimated to vary between 108 and 172 €/MWh, depending on the design of the farm [3,35].

According to the report on the state of Chile's wind energy by the *Centro nacional para la Innovación y Fomento de las Energías Sustentables* [10] (2016), the total installed capacity by the end of February 2016 was ~960 MW, generating a total contribution of 24.03% within renewable energies. However, the total installed capacity is 4.6% of the system's current power, though all this power is attributable solely to onshore wind energy, where the highest capacity onshore wind farms in Chile are: “El Arrayan” with 115 MW of power; “Los Cururos” with 110 MW; “Eólica Taltal” with 99 MW; “Talinay oriente” with 90 MW and “Valle de los vientos” with 90 MW, which were implemented between 2013 and 2015.

Several studies have analyzed onshore wind energy in Chile, such as Watts & Jara's statistical analysis [60]; wind power potential in the region of Maule [37], wind power potential in Magallanes [63] and the “Wind explorer” developed by the Department of Geophysics at the University of Chile.[1] However, knowledge about offshore wind power is still being developed. Some work has been done to enhance information regarding the status of offshore wind energy potential in Chile, from studies on synoptic climatology of

* Corresponding author. Av. Santa Rosa N° 11315, Santiago, Chile.
E-mail address: cmattar@uchile.cl (C. Mattar).

[1] http://walker.dgf.uchile.cl/Explorador/Eolico2/Description and user's manual at: http://walker.dgf.uchile.cl/Explorador/Eolico2/info/Documentacion_Explorador_Eolico_V2_Full.pdf.

http://dx.doi.org/10.1016/j.energy.2017.05.099
0360-5442/© 2017 Elsevier Ltd. All rights reserved.

near-surface wind [45] to preliminary studies on the wind power off Chile's coastline, estimated at no less than 150 km from the coast [31] and, specifically, off the coast of the Maule Region [30].

The above-mentioned work notwithstanding, there has yet to be an analysis on the technical and economic feasibility of using Chile's offshore wind power, as well as the potential costs of using it to generate electrical power. In addition, these new energy sources are in accordance with Law 20.698, which promotes expanding Chile's energy array by using renewable sources to reach a set target of 20% renewable energy by 2025 [28]. Therefore, the aim of this paper is to analyze the technical and economic feasibility of offshore wind power density in order to supplement existing information and encourage the implementation of such projects, with an eye to increasing the share of renewable energies supplying the country's energy array. The structure of this paper is as follows: Section 2 describes the study area and data used in this paper. Section 3 presents the methodology used, Section 4 the results and analysis, Section 5 the discussion of this work, and finally Section 6 presents the conclusions.

2. Study area, data and method

2.1. Study area

The study area consists of the region comprised of Chile's coastal border and 100 km to the west over the Pacific Ocean, and from 18° S to 56°S latitude (Fig. 1). It is important to point out that this area compliments the study carried out by Mattar and Villar-Poblete [31] in estimating wind energy power thanks to the better spatial resolution of the data used in this paper. This area of study is characterized by the presence of the southeastern Pacific's subtropical anticyclone, which directs wind toward the equator along most of Chile's coastline. At the same time, seasonal changes in wind speed in this area are produced largely by latitudinal changes in the wind component [45].

2.2. Data

2.2.1. Reanalysis ERA-Interim

ERA-Interim reanalysis is a sequential data assimilation system generated by the *European Centre for Medium-Range Weather Forecasts* (ECMWF), where for each 12-h analysis cycle, the available observations are combined with information from a forecast model in order to estimate the evolving state of the global atmosphere and its underlying surface [13].

The data used in this study are time series of wind speed data. There were delivered in their components ($\vec{u}$, $\vec{v}$) via a global 0.125° × 0.125° grid [13]. These data include a time series from 1979 to 2014 at a temporal resolution of 3 h, delivered for a height of 10 m above sea level.

Wind data provided by ERA-Interim have been widely used, tested and validated in numerous studies on atmospheric parameters, including analyses and simulations of wind fields in different areas of the world and for the estimation of offshore wind energy power [1,2,4,7,29,30,38,50–53,8,9,55].

This demonstrates that values delivered by ERA-Interim are a valid source of data for analyzing such general atmospheric circulation patterns as wind speed and direction, as well as offshore wind power.

2.2.2. Economic data

The economic information used to estimate costs and profitability was compiled from prior work provided by Myhr et al. [35]. and Moné et al. [36]. In addition, based on these studies, it was divided into five project stages, which appear in Table 1 and take into consideration three possible rated capacities for a potential offshore installation: 80, 160 and 240 MW.

The project's Life Cost Cycle Analysis (LCCA) is described below according to [35].):

- Prior studies and planning; given by environmental studies on seabed, interface and engineering design, plus management services and project development.
- Production and acquisition, which looked at the value of the turbines, the infrastructure to be used as determined by the particular seabed location and depth, the mooring system or anchoring, and finally the cost of connecting to the network (including the cost of necessary marine cable as a function of the distance to the coast).
- Installation and commissioning, including costs of installing floating wind turbines, installing the mooring system and installing necessary electrical infrastructure.
- Operation and maintenance costs given for staff and equipment and ships needed for maintenance.
- End of project and decommissioning, corresponds to costs arising from the process of dismantling and removing parts, taking them back to land to be recycled later or sold as scrap.

2.3. Method

2.3.1. Estimation of the wind power density

The magnitude of wind speed on each pixel was obtained using the following equation:

$$V = \sqrt{\vec{u}^2 + \vec{v}^2} \quad (1)$$

where, V is the magnitude of wind speed at a height of 10 m (m/s); $\vec{u}$ is the wind component u (East-West) and $\vec{v}$ is the wind component v (North-South). This was done over the entire time series and all pixels of the study area. Then, the wind speed was extrapolated at a height of 140 m, matching the size of the V164–8.0 MW wind turbine (Supplementary 1), which was chosen for this evaluation because it was installed at the Østerild test center in Denmark, where it produced 192,000 kWh of electricity generated in a 24 h period,[2] the most powerful commercial wind turbine currently available on the market. For extrapolation, equation (2) was applied, which requires a roughness length factor (Z_0) that was estimated according to surface type. In this case, a Z_0 was used, which corresponds to 0.0002 m, the value established for the sea surface [62].

$$V_z = V_i \frac{ln\left[\frac{Z_Z}{Z_0}\right]}{ln\left[\frac{Z_i}{Z_0}\right]} \quad (2)$$

where, V_z is the estimated wind speed at height Z_Z (m/s); V_i is the wind speed at the height for which data are available (m/s); Z_Z is the height at which the wind speed is being estimated (m); Z_0 is the surface roughness length (m) and Z_i is the height for which data are available (m).

To determine the probability of wind events, the Weibull probability density function (3) is used and has been applied in other studies to determine wind power in other geographical areas [12,20,24,25,43,48,61]. To do this, the method of least squares was used, which ascertained the values *A*, which is the slope, and *B*,

[2] http://www.vestas.com/%7E/media/vestas/investor/investor%20pdf/financial%20reports/2014/ar/2014_ar_technology%20and%20service%20solutions.pdf.

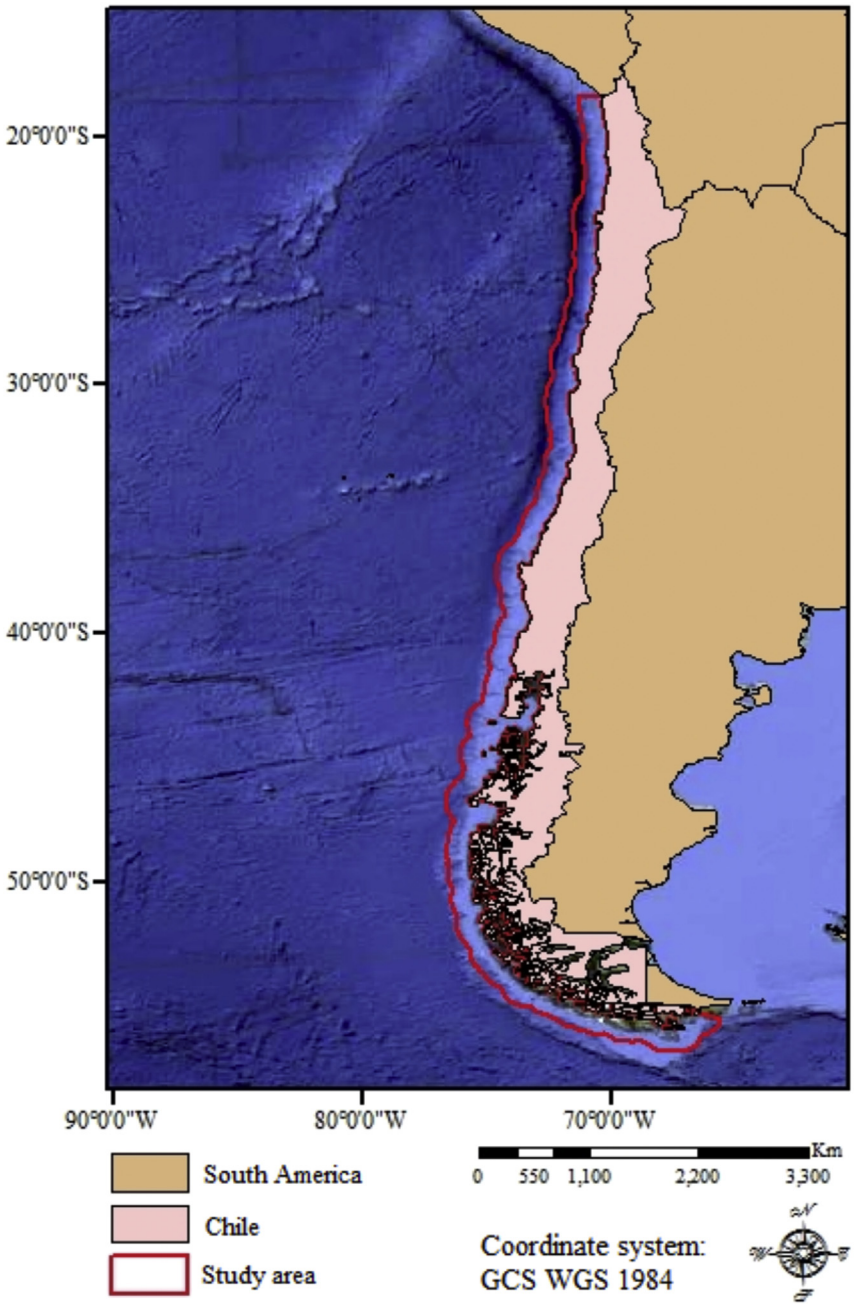

Fig. 1. Study area for the calculation of wind energy potential.

which is the intercept of the linear regression, and with which the factors *alpha* (α) and *beta* (β) (4) are ascertained in order to be able to calculate the Weibull probability density.

$$p(V_z) = \left(\frac{\beta}{\alpha}\right) \times \left(\frac{V_z}{\alpha}\right)^{\beta-1} \times e^{-\left(\frac{V_z}{\alpha}\right)^{\beta}} \tag{3}$$

$$\alpha = e^{-\frac{B}{A}}; \beta = a \tag{4}$$

where, V_z is the wind speed, α is the scale parameter and β is the shape parameter.

From the probability density curve and wind speed data, wind energy potential was calculated using equation (5), which gives the average wind power density for the desired period of time. The air density used was the wind industry's standard reference measurement, which at normal atmospheric pressure and at 15 [° C] is 1.225 [kg/m^3].

$$\frac{P}{A} = \frac{1}{2}\rho \int_0^{\infty} V^3 p(V_z) dV \tag{5}$$

where, P/A is the wind power density; P is the wind power (W); A is the swept area (m^2); ρ is the air density (Kg/m^3); $p(V_z)$ is the wind

[3] www.minenergia.cl.

Table 1
Costs considered for different project stages for different installed capacities.

Stage	Description	80 MW (USD)	160 MW (USD)	240 MW (USD)
Prior studies and planning	Environmental studies and station	4,780,127	8,100,713	11,028,811
	Studies of seabed	860,423	1,458,128	1,985,186
	Engineering design	111,855	189,557	258,074
	Project management and development	59,283	100,465	136,779
Production and acquisition	Turbine	132,800,000	265,600,000	398,400,000
	Infrastructure	57,509,248	115,018,496	172,527,744
	Mooring or anchor	7,081,018	14,162,037	21,243,055
	Network connection	28,932,995	57,865,990	86,798,985
Installation and commissioning	Wind turbines	12,086,168	24,172,336	36,258,504
	Electrical Infrastructure	13,413,047	17,096,770	20,780,493
	Marine Cable[a]	395,883	395,883	395,883
Operation and maintenance	Operation	3,200,000	6,400,000	9,600,000
	Maintenance	6,000,000	12,000,000	18,000,000
End of project	Decommissioning	10,220,990	20,402,391	30,583,793

[a] Cost set for 1 km. This cost is not fixed in the analysis, because it is varied as a function of the distance from the coast of each pixel.

probability density and V_z is the magnitude of the wind speed (m/s).

So, to determine the energy, the following equation was used:

$$E = T \int_0^{\infty} p(V_z) P(V_z) dV_z \tag{6}$$

where, $p(V_z)$ is the Weibull probability density function for the time period T; $P(V_z)$ is the wind turbine's power output at a determined wind speed (wind turbine curve) and T is the time period under study (hours).

2.3.2. Capacity factor and performance

The technical feasibility analysis is the estimated wind energy potential and its relation to energy production, based on the power curve for the V164–8.0 MW wind turbine. This was done on each pixel (spatial unit of 16 × 16 km in the study area). From this power curve model, the capacity factor (7) was calculated. This factor is defined as the ratio of the wind generation produced by the turbine and the total generation it outputs at full capacity over a period of time [25].

$$CF = \frac{PE}{PN{*}T} \tag{7}$$

where, CF is the capacity factor; PE is the estimated output; PN is the rated output and T represents time. In addition, the wind turbine's annual seasonal performance was estimated, (8) which is given by the ratio between the energy produced and the energy possessed by the wind [59].

$$\eta EST = \frac{E}{E_d} = \frac{P}{P_d} \tag{8}$$

Where, ηEST is the wind turbine's seasonal performance; E is the wind energy produced; E_d is the available wind energy; $\langle P \rangle$ is the functioning turbine's annual average useful potential, and $\langle P_d \rangle$ is the average annual wind potential available.

Generally, it is established that the range of values for an offshore wind farm's capacity for its effective approval may vary between 30% and 55% [56]. However, in this paper a capacity factor is considered feasible at 20% or higher, provided performance is greater than or equal to 10%. The reason for this is to show the relationship between the evaluated wind turbine and the wind energy power found. For this reason, economic indicators were applied only to pixels that fulfilled both requirements.

2.3.3. LCOE, NPV and IRR

To evaluate the economic profitability of an offshore wind farm in each pixel, three different scenarios were established for its installed capacity by using a generation unit equivalent to a wind farm of 80, 160 and 320 MW, respectively. The capacity for scenario 1 was determined with regard to what was used by the *National Renewable Energy Laboratory* (NREL) [26], while the capacity for scenarios 2 and 3 were determined in order to visualize the economic outcome at greater power output. These installed power outputs were evaluated economically for each 0.125° × 0.125° pixel across the study area. The evaluation applies the Levelized Cost Of Energy (LCOE) and cash flow in order to produce 3 economic indicators: the Net Present Value (NPV), Internal Rate of Return (IRR) and Pay-Back (PB). The initial assumptions established for the cost assessment with regard to the three scenarios of wind farms under evaluation are shown in Table 2.

To estimate the LCOE, the life cycle costs of power generation technology per unit of electricity (MWh) are evaluated [57]. This approach has been widely used to compare energy production technologies in terms of cost-effectiveness [6]. However, this tool depends on many parameters that are partially known or entail some uncertainties [5]. From this, the LCOE was obtained through the following equation:

$$LCOE = \frac{\sum_{t=0}^{n} \frac{I_t + M_t}{(1+r)^t}}{\sum_{t=0}^{n} \frac{E_t}{(1+r)^t}} \tag{9}$$

where, I_t represents the investments at time t; M_t is the maintenance and operating costs at time t; E_t is the energy generated at time t; r is the discount rate of the evaluation; and t is the time between zero up to the total number of years for which the project is being evaluated.

Incoming revenue is given by the evaluation of energy output with regard to capacity factor and the time value per MWh on the

Table 2
Characteristics under evaluation.

Characteristic	Value	Source
Wind turbine	Vestas V164–8.0 MW	–
Substructure	SPAR (Hywind-II)	Karimirad & Moan [23]
Installed power	80 MW/160 MW/240 MW	–
Number of turbines	10/20/30	–
Water depth	200 m	Myhr et al. [35]
Years of operation	25	Vestas [58]

international market. This value was set at 110 USD/MWh, based on the average price paid in countries like Germany, Portugal and Italy [16], bearing in mind they possess incentive schemes for renewable energy generation. In addition, the cash flow for each pixel considered the direct profit between investment and the price per MWh for offshore wind energy on the international market, which provided three economic indicators for the project's feasibility, as detailed below.

The NPV is the present value of the incoming and outgoing cash flow from the investment, and thus shows the total benefit to be derived from the investment in a project, which is obtained by the following equation [27]:

$$NPV = \sum_{t=0}^{N} \frac{FC_t}{(1+r)^t} \tag{10}$$

where, FC_t is the cash flow for a specific time period; r is the discount rate and t is the time from zero up to the number of years the project lasts. The result served as a criterion as to whether to carry out the project: if NPV> 0, this indicates the project should be carried out, if NPV = 0, nothing is gained or lost by carrying out the project, and if NPV <0, the project is not profitable. The IRR (11) is the rate of return or internal rate of return of an investment, and as such, shows an investment's profitability [27].

$$NPV = \sum_{t=0}^{N} \frac{FC_t}{(1+\boldsymbol{IRR})^t} = 0 \tag{11}$$

where, *NPV* is the net present value; *IRR* is the internal rate of return; *FC* is the cash flow for the year *t*, which is the time period in years that the project lasts. Finally, the PB (12), is the period in which the cost of the initial investment is recovered through annual cash flows [27].

$$PRC = \sum_{i=0} FCi = 0 \tag{12}$$

where, *FCi* is the cash flow in the year *i*.

In this paper, the NPV, IRR and PB values were estimated using a project evaluation horizon of 25 years, which corresponds to the lifespan set for the V164–8.0 MW model and is consistent with the measurement estimated for a wind farm [19]. In addition, a discount rate of 10% was applied, in accordance with the Chilean Ministry of Energy's wind energy projects[3] and a category one tax rate of 19%. In addition, two scenarios were considered regarding investment, the first based on an investment of 100% and the second taking into consideration a subsidy of 15%.

3. Results and analysis

3.1. Wind power density

Fig. 2 shows the mean seasonal variation (1979–2014) of wind speed (m/s) at 10 m above sea level. The minimum value obtained was recorded in the month of May (1.15 m/s) and the maximum value in November (12.8 m/s). From 18 to 28°S, it has lower average speeds than it does in the rest of the country (~4 m/s). A seasonal pattern corresponding to an increase of, on average, 2 m/s between 31 and 42°S can be observed between May and July. During the austral summer months of December, January and February (DJF), an area of maximum speed is seen between 29 and 39°S. Moreover, the southern zone exhibits its maximum monthly wind speed, although this area is difficult characterize due to its connectivity (eg. islands and archipelagos). These patterns resemble those in the Rahn & Garreaud study [45]; though in that paper, wind speed patterns were characterized bi-monthly, thus reducing the relative monthly maximum presented in said work by ~ 2 m/s.

Fig. 3 shows the range of average speed between 1979 and 2014 estimated at a height of 140 m, which goes from 1.56 m/s to 15 m/s, with a maximum standard deviation of 5.78 m/s, the minimum speed found for the period under study is near zero and the maximum wind speed is 53.1 m/s. Maximum speeds of 40 m/s can be observed in some areas between 52 and 56°S, which is in the extreme south of the country. In the area from 16 to 21°S falling inside the first 100 km from the coastline, wind speed does not appear to have a large amplitude due to the small difference between the maximum and minimum speeds. Meanwhile, in the southern region from 49 to 56°S, speeds are higher as compared to those in the rest of the country.

Fig. 4 shows the parameters of the Weibull distribution, the scale parameter, *alpha* (4.a), which ranged from 1.76 to 16.99, and the shape parameter, *beta* (4.b), which ranged from 1.30 to 6.86. The *alpha* parameter usually has a shape that is similar to the average, as it does in this study, where a slight increase can be seen between 28 and 43°S. In turn, the *beta* parameter shows minimum values in the area of around 20°S due to the difference between the maximum and minimum wind speed. South of 20°S, the beta value gradually decreases to 30°S due to a possible wind transition zone off the coast of Chile. To the south of 30°S, there is no visible characteristic pattern of *beta* associated with any variation in the maximum and minimum speeds.

Wind power density shows a range from 3.9 W/m2 to 3190 W/m2, while wind potential goes from 0.08 MW to 67.4 MW, and production from 0.005 GWh to 54.7 GWh (Fig. 5). On the maps, it can be observed that from 45° to 56°S, the values are at their highest, reaching 3190 W/m2, as does production from 41.1 GWh to 54.7 GWh. It can be further noted that from 28 to 41°S, there is a significant longitudinal increase in wind power density and production. On the other hand, the lowest values for production are mainly found from 18 to 28°S, which range between 6.0 GWh and 18.0 GWh. The offshore wind power density found in ~90% area of study can be assigned a class equal to or greater than 3, according to the wind power classification established by the *National Renewable Energy Laboratory* (NREL).[4] A classification of 3 or higher can be considered suitable for the installation of various commercial turbines [49].

Moreover, compared to previous studies that estimated offshore wind power in the corresponding area off the coast of the Maule Region (34–36°S), developed by Mattar & Borvarán [30]; it is possible to note that there were differences, on average, <2 m/s, which may be related to the fact that in said study, the wind fields were modeled at a resolution of 3 × 3 km and using one year of data. In this work though, 36 years of data were used at a spatial resolution of 16 × 16 km, thus attributing any differences to the spatial resolutions used in the two studies. Nevertheless, in this work, similar results are shown for both the Weibull parameters (alpha and beta) as well as for production, which is probably attributable to the same seasonal wind pattern.

If this is true, the area with the greatest wind power is located between 50 and 56°S due to the high speeds in this area, though it is unlikely that this potential might be exploited using the technology evaluated for this study. In this area, the minimum speeds exceed the cut-in speed of the wind turbine evaluated in this study (V164–8.0 MW), which equals 4 m/s, while its maximum speeds do not exceed the estimated cut-out speed of 25 m/s, which would imply a continuous use of the turbine. In addition, the average

[4] http://rredc.nrel.gov/wind/pubs/atlas/tables/A-8T.html.

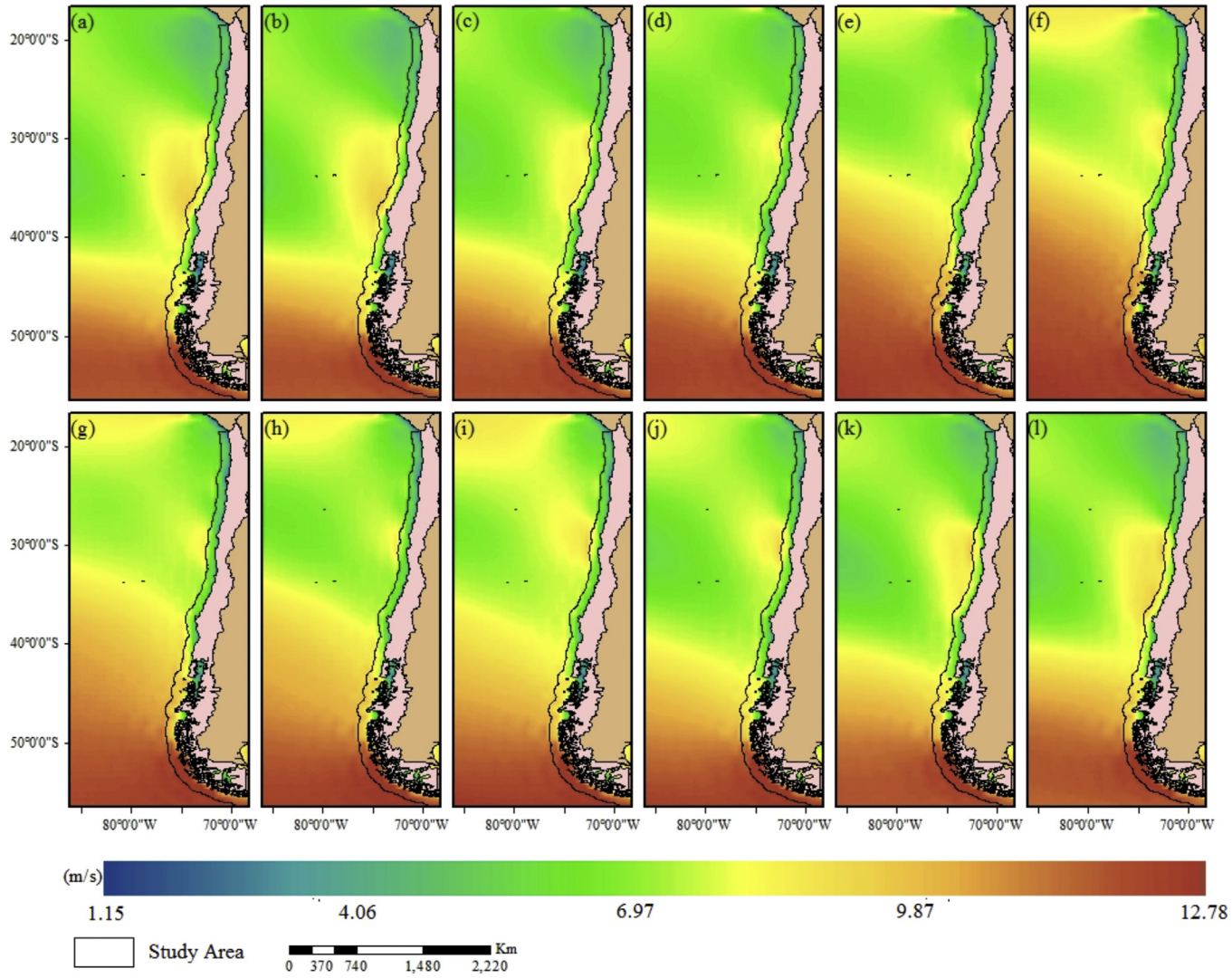

Fig. 2. Mean monthly long term wind speed values (10 m). January (a), February (b), March (c), April (d), May (e), June (f), July (g), August (h), September (i), October (j), November (k), December (l).

speeds of this area are similar to the wind turbine's rated output speed (13 m/s), which could lead to material fatigue, thus shortening its lifespan [39]. Finally, Fig. S2 (Supplementary 2) shows the variation of wind energy potential according to roughness length; this only shows significant variations to the south of 50°S.

3.2. Technical feasibility

In the study area, the obtained capacity factor fluctuates between 0.008% and 78.1%, while the performance oscillates between 0.8% and 43.6%, as shown in Fig. 6, where the inverse relationship between these two indicators can also be seen. The capacity factor consistent with previous results is higher between 45 and 56°S, where a wind turbine used for this study would operate at full capacity for most of the year, achieving values to a great extent >60% However, these values exceed the operating limits for the type of wind turbine selected for this work. Moreover, the performance is low in this area, with values < 24%, because the potential of the turbine under evaluation cannot effectively use this high wind power. From 18 to 25°S, the best performance at nearly 40% can be seen, in contrast to capacity factor values of <30%. Notably, the area between 28 and 32°S shows capacity factor values between 40% and 60% and performance between 27% and 35%, which are considered close to the technical balance between the two parameters. This zone coincides with the greatest onshore wind generation, thus making this highly suitable for a mixed farm of on- and offshore wind energy.

Fig. 7 shows the areas that are evaluated economically according to their technical feasibility, which is based on capacity factor and performance, using thresholds of 20% and 10%, respectively. It can be seen that the areas feasible according to these two criteria range from 27 to 47°S, and an area not technically feasible for the wind turbine evaluated in this study to the north of 20°S. Moreover, Fig. 7 b shows no technical feasibility to the south of 50°S due to poor performance from the wind turbine in this area. In addition, this range of feasibility associated with a range greater than 20% capacity factor and performance, is limited for the areas at the two ends of the study area. In the case of Fig. 7c, a large proportion of the areas close to the coast that had a high wind power would fall in a zero technical feasibility category, as can be seen at 30 and 40°S. All the economic analyses described in the next section were made based on Fig. 7 a (Capacity factor $\geq$ 20% and $\geq$10% performance). Previous studies have proven the use of these technical indicators, with which wind projects of this kind in Europe have been carried out [47].

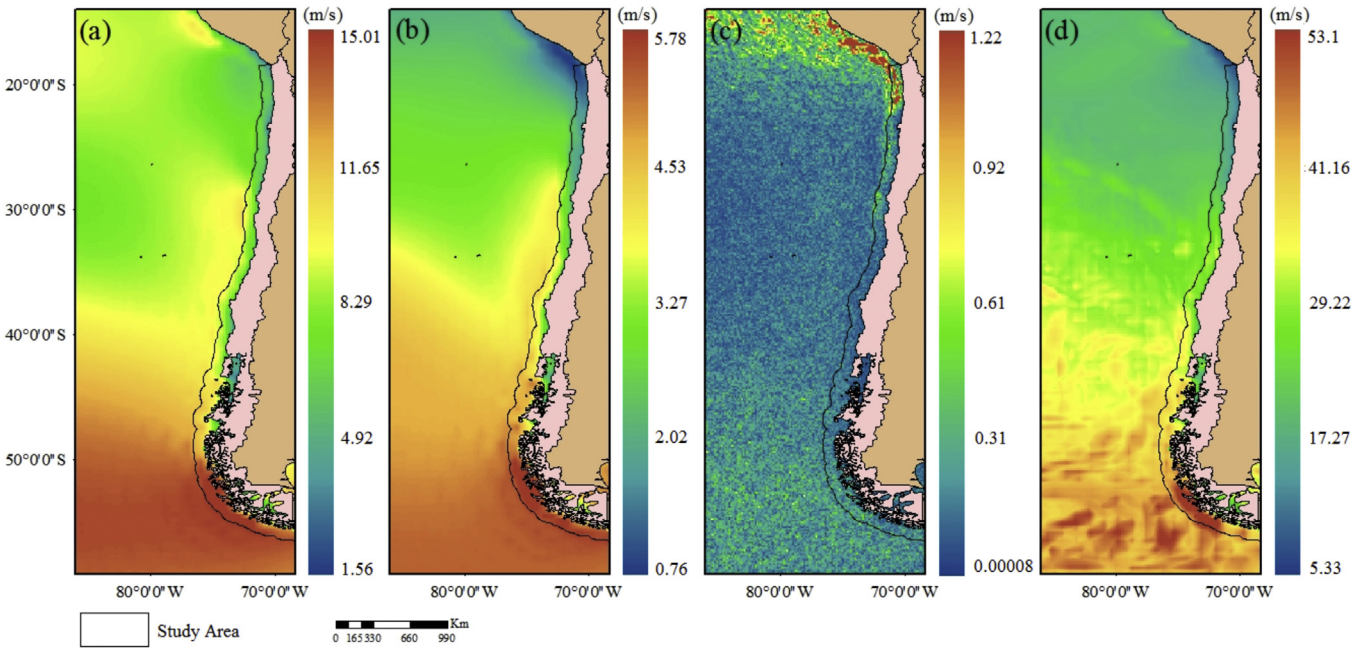

Fig. 3. Mean (a), standard deviation (b), minimum (c) and maximum (d) of wind speeds extrapolated at height of 140 m.

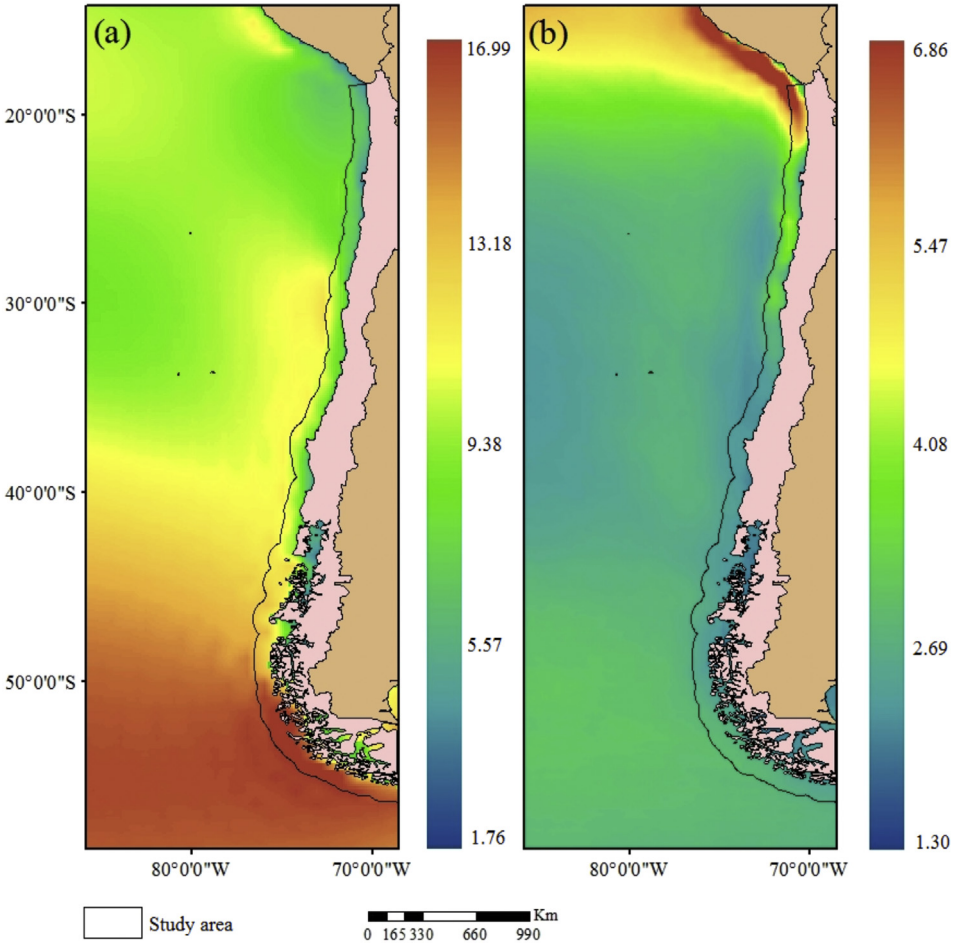

Fig. 4. Weibull parameters; Alpha, (a) and beta (b).

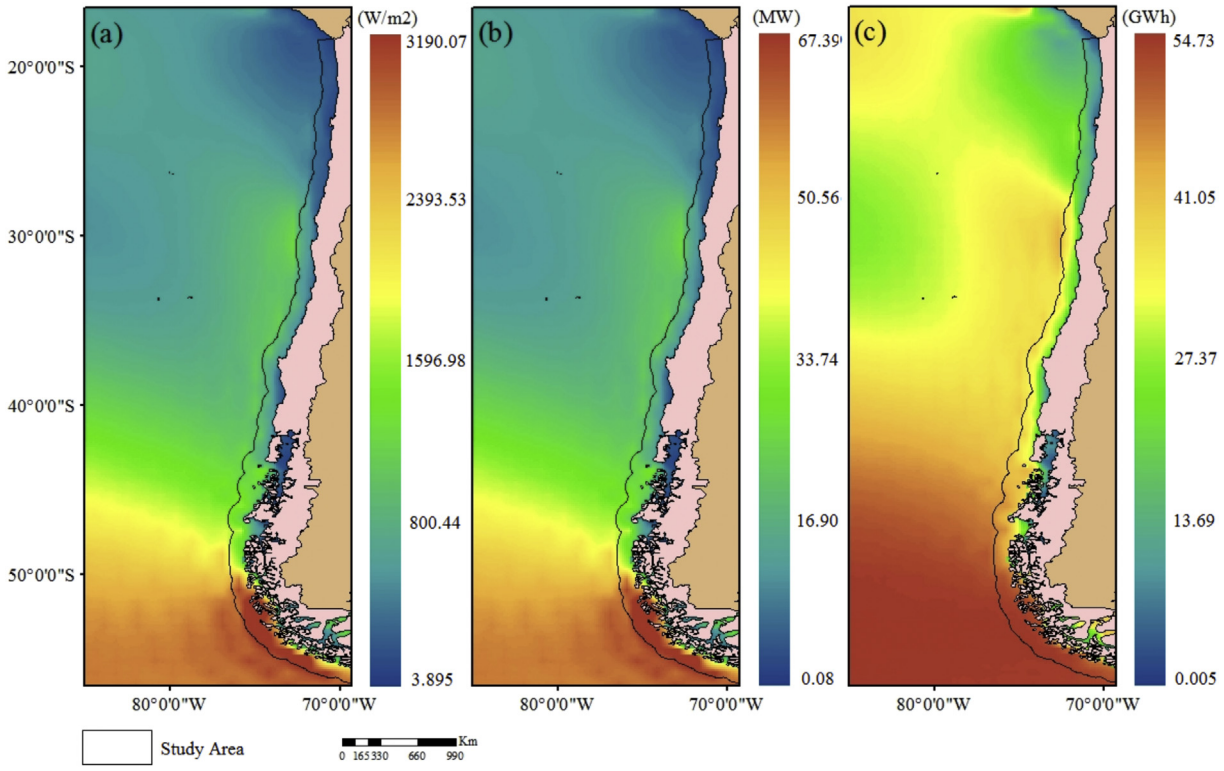

Fig. 5. Power density (a), wind power (b) and production (c).

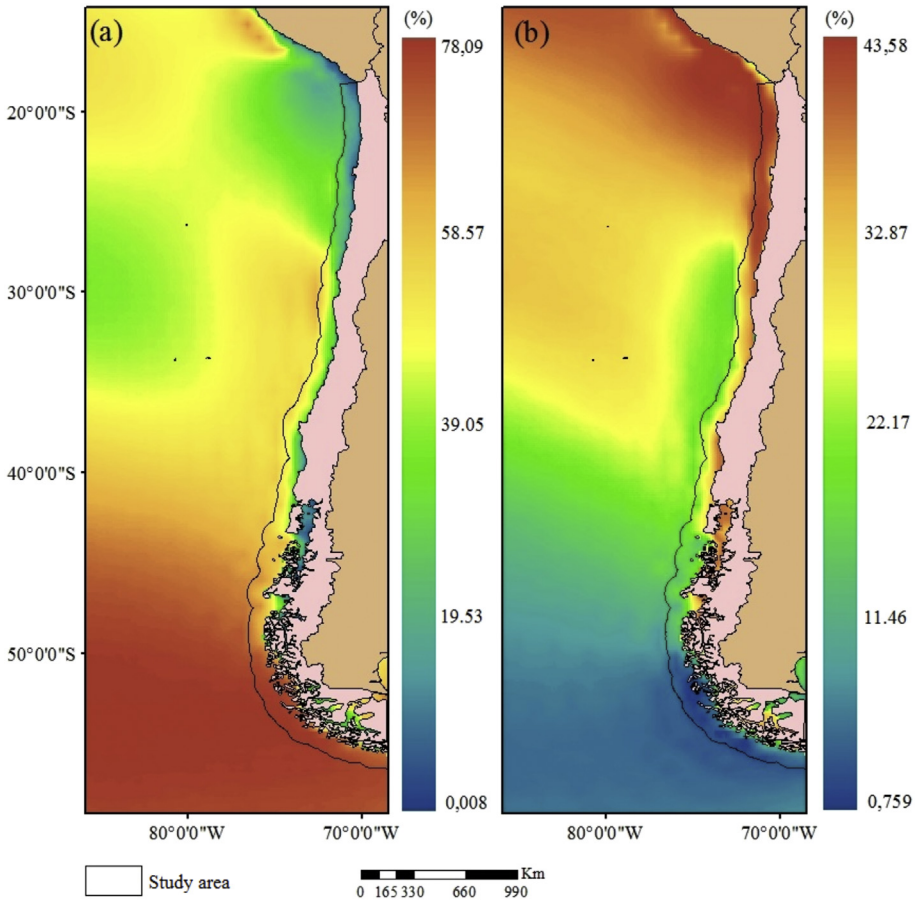

Fig. 6. Capacity factor (a) and performance (b).

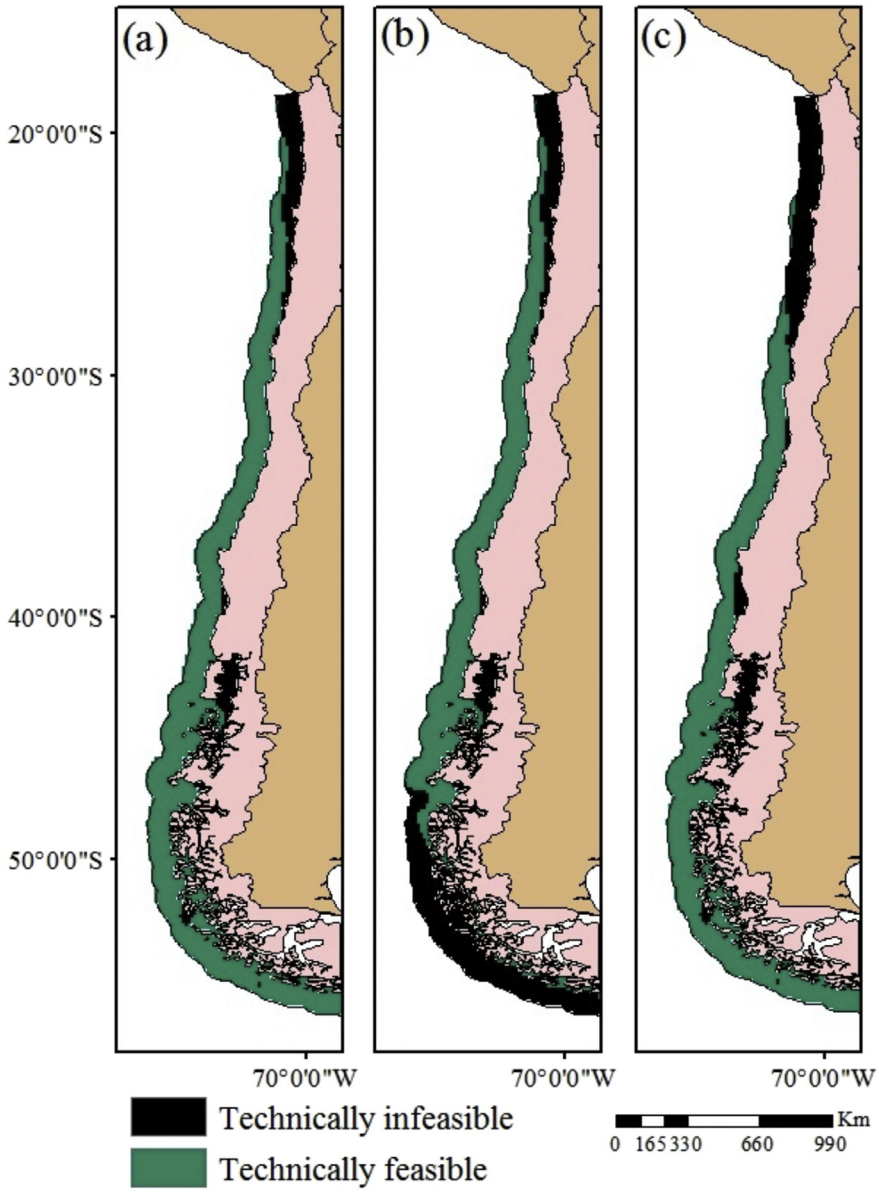

Fig. 7. Technical feasibility for the offshore wind power in the study area. Different scenarios by varying the percentage of capacity factor and performance. a) CF ≥ 20% and ≥ Performance 10%. b) CF ≥ 20% and ≥ Performance 20%. c) CFP ≥30% and ≥ Performance 10%.

3.3. Economic feasibility

Table 3 shows the minimum and maximum amounts of investments for the different installed capacity scenarios of the wind farm. Depending on how far from the coast it is located, the cost can increase due to the length of the marine cable. On the other hand, it can be seen that the investment is not proportional to the size of the plant, as there are costs whose value per MW decreases as the size of the farm increases.

To estimate the LCOE, Fig. 8 shows three scenarios of installed capacity, corresponding to 80, 160 and 240 MW. In general, the LCOE values range between 100 and 140 USD $/MWh between 30 and 45°S. To the south of this area, between 46 and 56°S, are the lowest LCOE values, ranging between 71 and 100 USD $/MWh. However, north of 30°, LCOE values exceed 200 USD $/MWh, making it a non-competitive scenario for the Chilean electricity market. Regardless, the LCOE estimates for part of the study area are economically competitive according to the study by *Bloomberg New Energy Finance* [18], in which LCOE values for renewable energies range from 33 to 178 USD$/MWh.

Table 3
Minimum and maximum investment by farm size.

Investment	Installed Power		
	80 MW	160 MW	240 MW
	(USD$)	(USD$)	(USD$)
Minimum investment	287,636,166	550,483,275	810,877,604
Maximum investment	337,956,684	600,803,792	861,196,693

The LCOE was estimated starting at a discount of 10%, although the impact of an increase in the discount rate to 12% on LCOE is significant for the three scenarios of installed power capacities of 80, 160 and 240 MW (Fig. 9.). In this figure, the significant effect that the applied discount rate has on the analysis can be seen, since with a 2% increase, the LCOE would increase by more than three

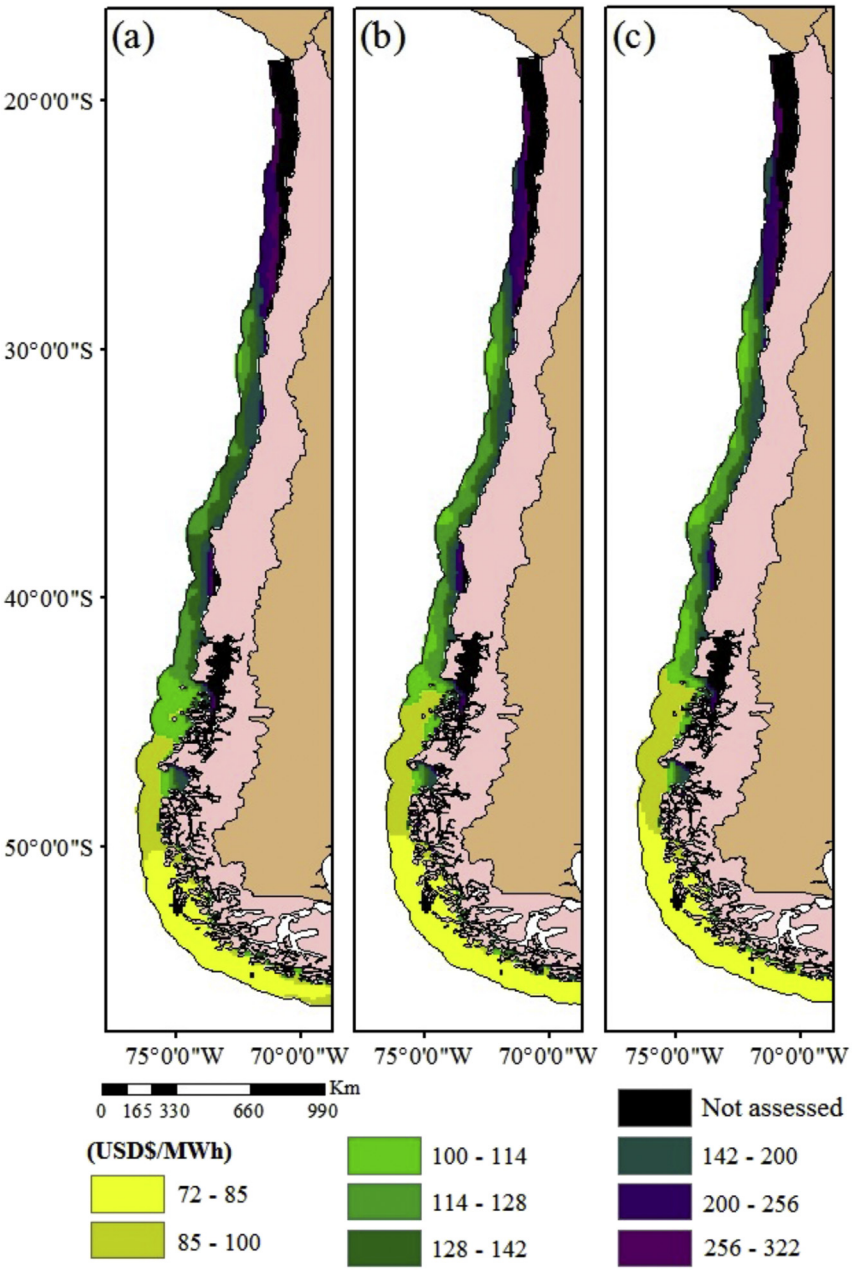

Fig. 8. Levelized cost of energy (LCOE) for the three scenarios under consideration with installed capacities; 80 MW (a), 160 MW (b) and 240 MW (c).

times its value, in both the minimum and maximum values observed for each of the scenarios described. Another attempt also used to evaluate energy projects is the Levelized Avoided Cost of Electricity (LACE), although the lack of information about financial and economic values related to the off-shore wind energy might retrieve a broad retrieval related to the off-shore cost of energy in Chile.

Fig. 10 shows the NPV for the base situation of a 100% investment and for an 85% investment, while also considering the size variations in the evaluated wind farms according to their respective installed capacities on a 25-year horizon. For the first case of investment (100%), it can be seen that irrespective of plant size, the positive NPV indicates that the project is feasible only between 43 and 56°S. However, when considering a second case of investment (85%) it is possible to observe an additional area of feasibility for the

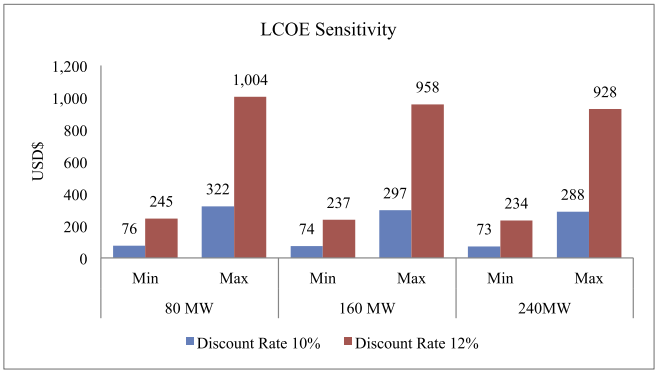

Fig. 9. LCOE sensitivity with regard to discount rate.

wind farm between 30 and 32°S. Under this same 85% investment scenario, it can be seen that the area south of 50°S gives an NPV ranging between 285 and 412 MUSD. In both investment cases, reducing the NPV has a significant impact due to the costs of wind farms for installed capacity over 160 MW, which is mainly evident in the area from 25 to 45°S.

A similar pattern to the one observed in the NPV can be seen in the IRR (Fig. 11), where feasible areas are those with a rate greater than or equal to the one evaluated (10%). The scenario of an 85% investment and an installed capacity of 240 MW gives the highest rate (~17%) and falls in the area ranging between 51 and 56°S. While between 18 and 29°S, the values are near zero or less than 2%, so these areas would be unfeasible for a wind project with the characteristics evaluated in this work. In the area between 30 and 32°S, rates close to 9% and 10% were estimated for investment cases corresponding to 100% and 85%, respectively, making them of interest for their economic feasibility. Lastly, Fig. 12 shows the PB, which follows spatial patterns similar to those seen above. From 18 to 30°S, no values for the return period were estimated, which means that it would take over 25 years to recover the investment. In the area between 30 and 45°S, the PB can change drastically, depending on the investment scenario and installed power in the different wind farms; PB close to 10 years can be seen for an 85% investment and installed capacity of 240 MW, and up to 20 years for 80 MW of power and 100% investment. Lastly, for southern latitudes between 45 and 56°S, the estimated PB is under 10 years, regardless of whether the initial investment is 100 or 85%.

4. Discussion

The offshore wind energy in Chile has never been technically evaluated due the lack in technology and costs barriers. However, the current worldwide energy scenario demonstrates the impact of offshore wind power in developed countries. This work tackles the new option to generate renewable energy along the coast of 6400 km in Chile which contribute to understand the new alternatives to assimilate and contribute to the diversification for the Chilean energy matrix. The costs of the offshore wind energy project evaluated in this study were estimated based on international market prices and installation assumptions such as depth. For this reason, it is necessary to adapt this information to local concerns by using studies of the seabed, which could affect the actual distance of the marine cable as well as the wind farm's underwater structure and the costs of reaching the installation site. Similarly, it is necessary to complement this work with new estimates of marine potential that would provide further detail of new

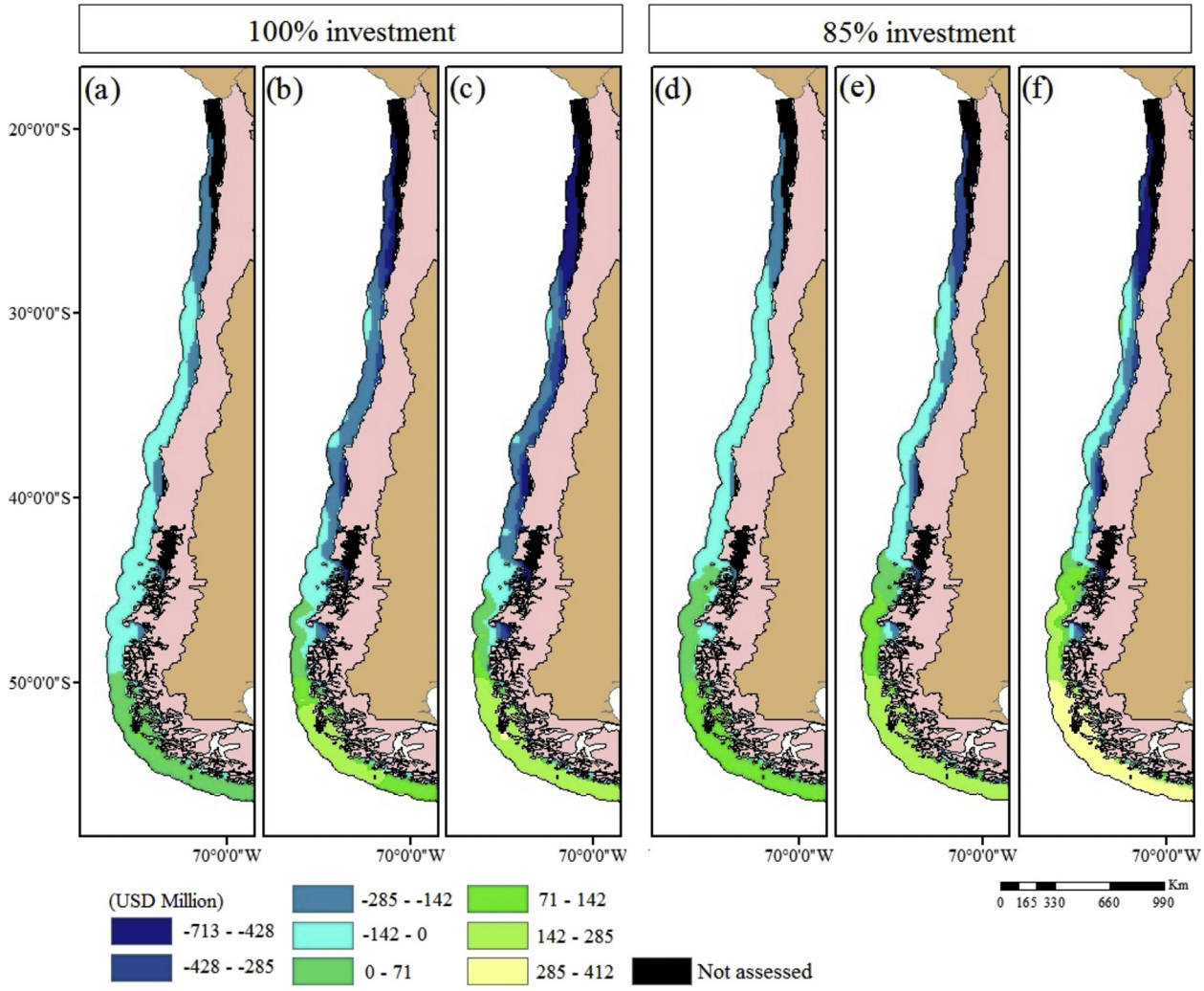

Fig. 10. NPV for base situation (100% investment) for farms at 80 MW (a), 160 MW (b) and 240 MW (c) and for the case of an 85% investment in farms at 80 MW (d), 160 MW (e) and 240 MW (f).

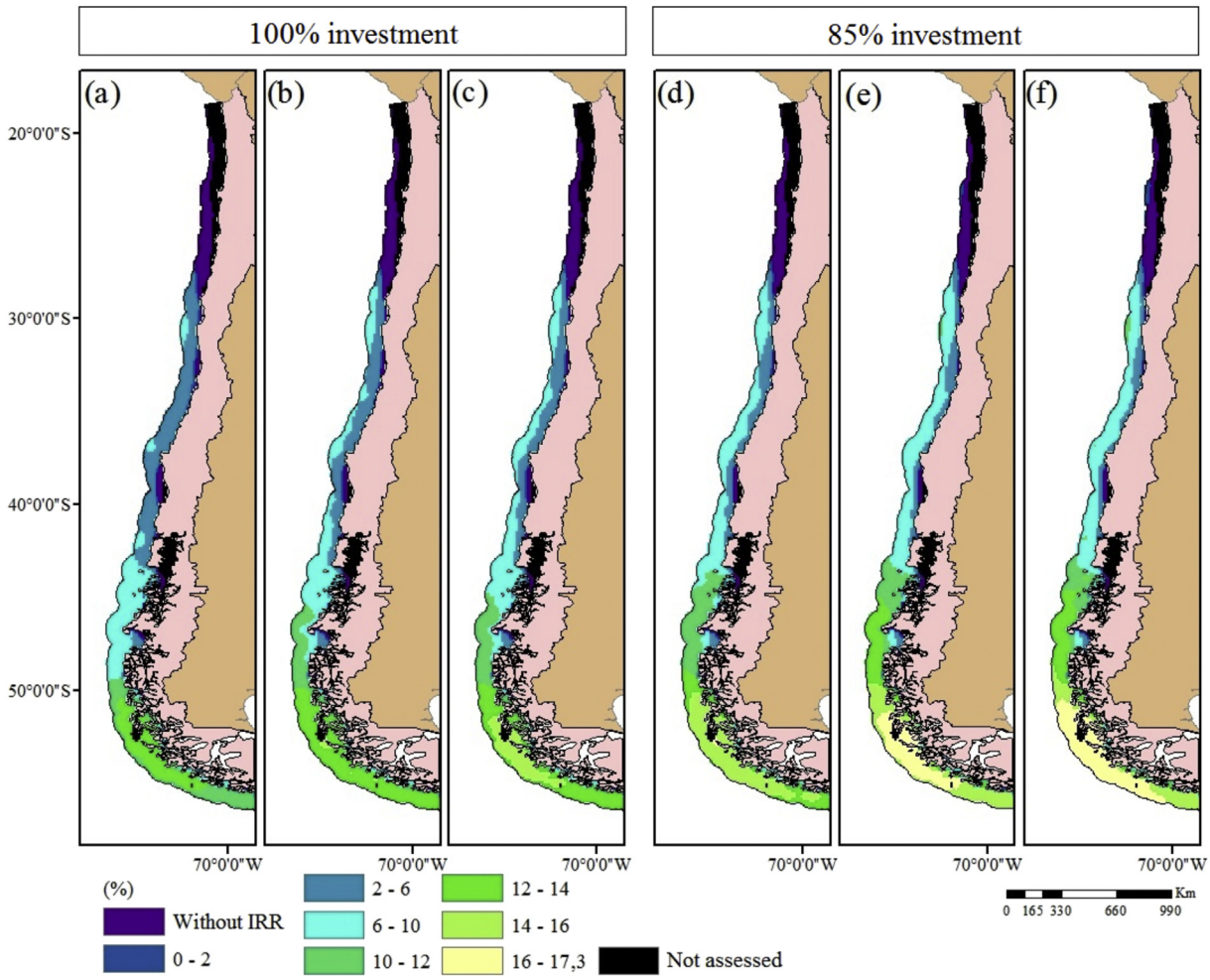

Fig. 11. IRR for base situation (100% investment) for farms at 80 MW (a), 160 MW (b) and 240 MW (c) and for the case of an 85% investment in farms at 80 MW (d), 160 MW (e) and 240 MW (f).

offshore energy sources that exist in Chile, as is the case for the work published by Mediavilla & Sepúlveda [32] on marine potential between 32 and 34.5°S. Additionally, the price of energy in Chile's energy system is set according to the marginal cost, which stems from the cost of generating one more unit of energy [41]. At present, there is no marginal cost for offshore wind energy, thus bringing about uncertainty as to the real impact that this technology would have on Chile's electricity market.

The investment in the wind projects evaluated in this study is similar to the costs presented by Myhr et al. [35] and NREL [36]. However, in Chile it gets particularly high when considering the existing regulatory framework for electricity production from renewable energy sources. This regulatory framework does not provide incentives on new technologies and does not ensure connection to power distribution systems, among others. Indeed, the transmission network in Chile can be also considered a barrier whether the connection node is far from the wind power supply. These barriers leads to some uncertainty as to the incorporation of offshore technology into Chile's energy array, thus limiting the diversification of sources of renewable energy and a dependence on international prices for this technology. One example is the feed-in-tariff (FIT) incentive scheme, which promotes the installation of renewable energy generators by ensuring their connection to the network and at a price based on its technology, thereby reducing uncertainty and risk [11]. Moreover, price uncertainties and forward price values can also be accounted in further offshore technology assessment.

One entry barrier to offshore wind energy is a lack of prospective offshore wind power studies and economic information about this energy source, which increases the risk for investment and identifying potential areas. It has been widely shown that these types of barriers to information limits the entry of new energy sources, thereby reducing diversification in generating it [15,46]. This work is a step toward making the first estimate of Chile's offshore wind power, and also exposes some possible technical and economic barriers that this energy might face in the future. For instance, the use of a better detailed bathymetric model in order to well defined the costs of the underwater cable or a turbulence model in order to adequate the energy generation results [33,34].

For the 85% investment evaluated in this work, which was obtained by reducing costs at various stages or from non-investor financial contributions, the implementation of an offshore wind farm is mostly profitable when installed in the area of the southern tip of Chile between 45 and 56°S, though the turbine could see its lifespan shortened. It is for this reason that the area ranging between 30 and 32°S stands out, as it shows feasibility in both investment cases (100 and 85%). Based on the data used in this study, the area between 18 and 28°S is not technically or economically feasible for developing an offshore wind farm because this area is characterized by its low potential as compared to the rest of study area.

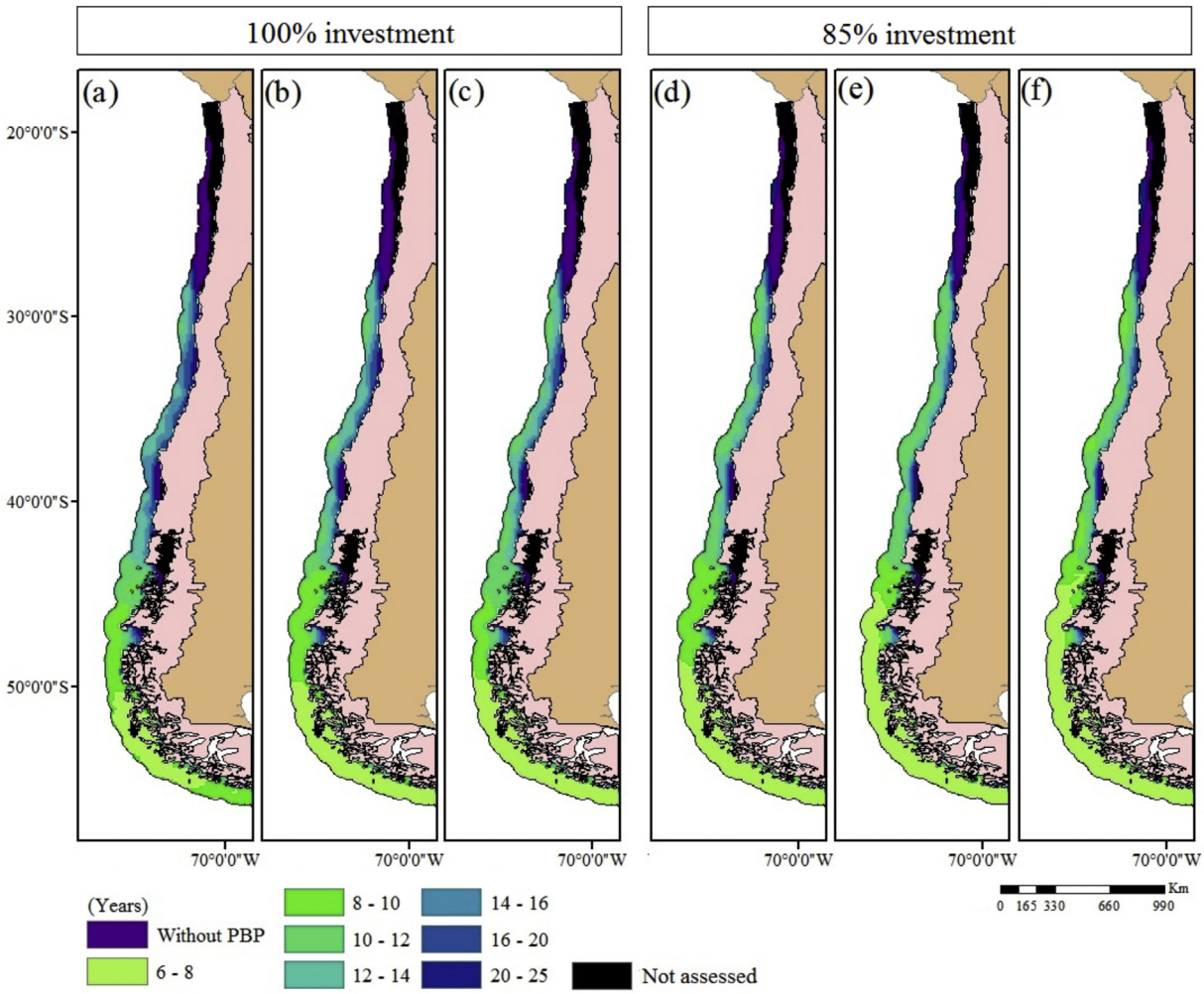

Fig. 12. PB for base situation (100% investment) for farms at 80 MW (a), 160 MW (b) and 240 MW (c) and for the case of an 85% investment in farms at 80 MW (d), 160 MW (e) and 240 MW (f).

5. Conclusions

For this paper, offshore wind power is estimated along Chile's coastline. In much of the study area, there are areas whose energy potential and consequent production are of great interest. The technical feasibility reveals that offshore wind energy has high capacity factors for the wind turbine under evaluation. The economic feasibility shows that the area between 45 and 56°S shows the lowest LCOE, between 72 and 100 USD$/MWh, as well as profitable values for NPV, IRR and PB. However, it should be kept in mind that this area's high power density requires the use of larger capacity turbines or turbines suited for the speeds that occur in these areas for optimal use.

The area of greatest potential interest when considering the technical and economic assessment is the area between 30 and 32°S because it has wind power density (between 700 W/m2 900 W/m2) and technical conditions (capacity factor between 40% and 60% and performance between 27% and 35%) necessary for carrying out the project as a function of the wind turbine under evaluation. The LCOE fluctuates between 100 and 114 USD $/MWh, which might be considered a competitive price in Chile's current electricity market. Lastly, this paper shows the first estimate of Chile's offshore wind power by taking into account some technical, economic and financial aspects that should receive further attention in order to make the most of this new source of renewable energy.

Acknowledgments

The authors would like to thank the ECMWF for providing the ERA-Interim data.

This paper was partially funded by the “Programa de Estímulo a la Excelencia Institucional (PEEI)”-University of Chile (271016).

Appendix A. Supplementary data

Supplementary data related to this article can be found at http://dx.doi.org/10.1016/j.energy.2017.05.099.

References

[1] Akhil S, Venkat M, Narayana D, Krishna B. Vertical distribution of ozone over a tropical station: seasonal variation and comparison with satellite (MLS, SABER) and ERA-Interim products. Atmos Environ 2015;116:281–92.
[2] Bao X, Zhang F. Evaluation of NCEP–CFSR, NCEP–NCAR, ERA-interim, and ERA-40 reanalysis datasets against independent sounding observations over the tibetan plateau. J Clim 2012;26:206–14.
[3] Bilgili M, Yasar A, Simsek E. Offshore wind power development in Europe and its comparison with onshore counterpart. Renew Sustain Energy Rev 2011;15:905–15.
[4] Boilley A, Wald L. Comparison between meteorological re-analyses from ERA-

Interim and MERRA and measurements of daily solar irradiation at surface. Renew Energy 2015;75:135–43.
[5] Boubault A, Ho C, Hall A, Lambert T, Ambrosini A. Levelized cost of energy (LCOE) metric to characterize solar absorber coatings for the CSP industry. Renew Energy 2016;85:472–83.
[6] Branker K, Pathak M, Pearce J. A review of solar photovoltaic levelized cost of electricity. Renew Sustain Energy Rev 2011;15:4470–82.
[7] Carvalho D, Rocha A, Gómez-Gesteira M. Ocean surface wind simulation forced by different reanalyses: comparison with observed data along the Iberian Peninsula coast. Ocean Model 2012;56:31–42.
[8] Carvalho D, Rocha A, Gómez-Gesteira M, Santos S. WRF wind simulation and wind energy production estimates forced by different reanalyses: comparison with observed data for Portugal. Appl Energy 2014a;117:116–26.
[9] Carvalho D, Rocha A, Gómez-Gesteira M, Santos S. Offshore wind energy resource simulation forced by different reanalyses: comparison with observed data in the Iberian Peninsula. Appl Energy 2014b;134:57–64.
[10] CIFES (Centro Nacional para la Innovación y Fomento de las Energías Sustentables). Reporte CIFES: energías renovables en el mercado eléctrico Chileno. March 2016 (tech. rep.) Santiago, Chile. 2016. p. 8. Available, http://cifes.gob.cl/documentos/reportes-cifes/reporte-cifes-marzo-2016/ [Accessed 20 June 2015].
[11] Couture T, Gagnon Y. An analysis of feed-in tariff remuneration models: implications for renewable energy investment. Energy Policy 2010;38:955–65.
[12] Dahbi M, Benatiallah A, Sellam M. Evaluation of wind power production prospective and Weibull parameter estimation methods for Babaurband, Sindh Pakistan. Energy Procedia 2013;36:179–88.
[13] Dee D, Uppala S, Simmons A, Berrisford P, Poli P, Kobayashi S, et al. The ERA-Interim reanalysis: configuration and performance of the data assimilation system. Q J R Meteorological Soc 2011;137:553–97.
[14] Dincer F. The analysis on wind energy electricity generation status, potential and policies in the world. Renew Sustain Energy Rev 2011;15(9):5131–42.
[15] Eleftheriadis IM, Anagnostopoulou EG. Identifying barriers in the diffusion of renewable energy sources. Energy Policy 2015;80:153–64.
[16] Fouquet D. Prices for renewable energies in Europe: feed in tariffs versus quota systems – a comparison. Report 2006/2007. Eur Renew Energies Fed 2007. Available, http://citeseerx.ist.psu.edu/viewdoc/download;jsessionid=F8C693F9C44A968925AB514C926E2D02?doi=10.1.1.189.4011&rep=rep1&type=pdf [Accessed 10 October 2015].
[17] Global wind report 2014 (tech. rep.). In: Fried L, Qiao L, Sawyer S, Shukla S, editors. GWEC (global wind energy Council). Brussels, Belgium; 2015. p. 76. Available, http://www.gwec.net/wp-content/uploads/2015/03/GWEC_Global_Wind_2014_Report_LR.pdf [Accessed 04 May 2015].
[18] Herrera C, Román R, Sims D. El costo nivelado de energía y el futuro de la energía renovable no convencional en Chile: derribando algunos mitos. NRDC. Nueva York, United States: NRDC (Natural Resources Defense Council); 2012. p. 31. Available, https://www.nrdc.org/laondaverde/international/files/chile-LCOE-report-sp.pdf [Accessed 06 May 2015].
[19] Igba J, Alemzadeh K, Durugbo C, Henningsen K. Through-life engineering services: a wind turbine perspective. Procedia CIRP 2014;22:213–8.
[20] Islam M, Saidur R, Rahim N. Assessment of wind energy potentiality at Kudat and Labuan, Malaysia using Weibull distribution function. Energy 2011;36:985–92.
[21] Kalogirou S. Wind energy systems. chapter. 13. In: Solar energy engineering. 2a Ed. United States: Processes and Systems; 2014. p. 735–62. 819.
[22] Kaplan Y. Overview of wind energy in the world and assessment of current wind energy policies in Turkey. Renew Sustain Energy Rev 2015;43:562–8.
[23] Karimirad M, Moan T. Feasibility of the application of a spar-type wind turbine at a moderate water depth. Energy Procedia 2012;24:340–50.
[24] Khahro S, Tabbassum K, Soomro A, Dong L, Liao X. Evaluation of wind power production prospective and Weibull parameter estimation methods for Babaurband, Sindh Pakistan. Energy Convers Manag 2014a;78:956–67.
[25] Khahro S, Tabbassum K, Soomro A, Liao X, Alvi M, Dong L, et al. A wind energy analysis of Grenada: an estimation using the 'Weibull' density function. Renew Sustain Energy Rev 2014b;35:460–74.
[26] Lantz E, Leventhal M, Baring-Gould I. Wind power project repowering: financial feasibility, decision drivers, and supply chain effects (tech. rep.). United States: National Renewable Energy Laboratory; 2013. p. 40. Available, http://www.nrel.gov/docs/fy14osti/60535.pdf [Accessed 25 May 2015].
[27] Lee CF, Lee AC. Encyclopedia of finance. United States: Springer Science & Business Media; 2006. p. 856.
[28] Ley 20,698. Propicia la ampliación de la matriz energética, mediante fuentes renovables no convencionales. Santiago: Biblioteca del congreso nacional de Chile; 2013. p. 4 [Publicada en Diario Oficial el: 22 de octubre de 2013].
[29] Linares A, Ruiz J, Pozo D, Tovar J. Generation of synthetic daily global solar radiation data based on ERA-Interim reanalysis and artificial neural networks. Energy 2011;36:5356–65.
[30] Mattar C, Borvarán D. Offshore wind power simulation by using WRF in the central coast of Chile. Renew energy 2016;94:22–31.
[31] Mattar C, Villar-Poblete N. Estimación del potential eólico "offshore" en las costas de Chile utilizando datos de escaterómetro y Reanalysis. Rev Teledetección 2014;41:49–58.
[32] Mediavilla DG, Sepúlveda HH. Nearshore assessment of wave energy resources in central Chile (2009–2010). Renew Energy 2016;90:136–44.
[33] Meng W, Yang Q, Ying Y, Sun Y, Yang Z, Sun Y. Adaptive power capture control of variable-speed wind energy conversion systems with guaranteed transient and steady-state performance. IEEE Trans Energy Convers 2013;28:716–25.
[34] Meng W, Yang Q, Sun Y. Guaranteed performance control of DFIG variable-speed wind turbines. IEEE Trans Control Syst Technol 2016;24:2215–23.
[35] Myhr A, Bjerkseter C, Agotnes A, Nygaard T. Levelised cost of energy for offshore floating wind turbines in a life cycle perspective. Renew Energy 2014;66:714–28.
[36] Moné C, Smith B, Maples B, Hand M. 2013 Cost of wind energy review (tech. rep.). United States: NREL (National Renewable Energy Laboratory); 2015. p. 94. Available, http://www.nrel.gov/docs/fy15osti/63267.pdf [Accessed 07 July 2015].
[37] Morales L, Lang F, Mattar C. Mesoscale wind speed simulation using CALMET model and reanalysis information: An application to wind potential. Renew Energy 2012;48:57–71.
[38] Nagababu G, Dharmil B, Kachhwaha SS, Savsani V. Evaluation of Wind Resource in Selected Locations in Gujarat. Energy Procedia 2015;79:212–9.
[39] Nejad A, Bachynski E, Gao Z, Moan T. Fatigue damage comparison of mechanical components in a land-based and a spar floating wind turbine. Procedia, Eng 2015;101:330–8.
[40] Oh K-Y, Kim J-Y, Lee J-K, Ryu M-S, Lee J-S. An assessment of wind energy potential at the demonstration offshore wind farm in Korea. Energy 2012;46:555–63.
[41] Palma R, Jiménez G, Alarcón I. Las Energías Renovables No Convencionales en el Mercado Eléctrico Chileno. CNE (Comisión Nacional de Energía), GTZ (German Technical Cooperation). Proyecto Energías Renovables No Convencionales (CNE/GTZ). Santiago, Chile: Cooperación Intergubernamental Chile-Alemania; 2009. p. 144. Available, http://www.cifes.gob.cl/archivos/ERNCMercadoElectrico_Bilingue_WEB.pdf [Accessed 15 October 2015].
[42] Perveen R, Kishor N, Mohanty S. "Offshore" wind farm development: Present status and challenges. Renew Sustain Energy Rev 2014;29:780–92.
[43] Pishgar-Komleh SH, Keyhani A, Sefeedpari P. Wind speed and power density analysis based on Weibull and Rayleigh distributions (a case study: Firouzkooh county of Iran). Renew Sustain Energy Rev 2015;42:313–22.
[44] Quan P, Leephakpreeda T. Assessment of wind energy potential for selecting wind turbines: An application to Thailand. Sustain Energy Technol Assessments 2015;11:17–26.
[45] Rhan D, Garreaud R. A synoptic climatology of the near-surface wind along the west coast of South America. Int J Climatol 2013;34:780–92.
[46] Richards G, Noble B, Belcher K. Barriers to renewable energy development: A case study of large-scale wind energy in Saskatchewan, Canada. Energy Policy 2012;42:691–8.
[47] Rodrigues S, Restrepo C, Kontos E, Teixeira R, Bauer P. Trends of offshore wind projects. Renew Sustain Energy Rev 2015;49:1114–35.
[48] Safari B, Gasore J. A statistical investigation of wind characteristics and wind energy potential based on the Weibull and Rayleigh models in Rwanda. Renew Energy 2010;35:2874–80.
[49] Shami S, Ahmad J, Zafar R, Haris M, Bashir S. Evaluating wind energy potential in Pakistan's three provinces, with proposal for integration into national power grid. Renew Sustain Energy Rev 2016;53:408–21.
[50] Shanas P, Sanil K. Comparison of ERA-Interim waves with buoy data in the eastern Arabian Sea during high waves. Indian J Mar Sci 2014;43(7):4.
[51] Škerlak B, Sprenger M, Wernli H. A global climatology of stratosphere–-troposphere exchange using the ERA-Interim data set from 1979 to 2011. Atmos Chem Phys 2013;14:913–37.
[52] Soares P, Cardoso R, Miranda P, Medeiros J, Belo-Pereira M, Espirito-Santo F. WRF high resolution dynamical downscaling of ERA-Interim for Portugal. Clim Dyn 2012;39:2497–522.
[53] Stopa J, Cheung K. Intercomparison of wind and wave data from the ECMWF Reanalysis Interim and the NCEP Climate Forecast System Reanalysis. Ocean Model 2014;75:65–83.
[54] Sun X, Huang D, Wu G. The current state of offshore wind energy technology development. Energy 2012;41:298–312.
[55] Szczypta C, Calvet J, Albergel C, Balsamo G, Boussetta S, Carrer D, et al. Verification of the new ECMWF ERA-Interim reanalysis over France. Hydrol Earth Syst Sci 2011;15:647–66.
[56] Tegen S, Lantz E, Hand M, Maples A, Smith A, Schwabe P. 2011 cost of wind energy review (tech. rep.). United States: NREL (National Renewable Energy Laboratory); 2013. p. 35. Available, http://www.nrel.gov/docs/fy13osti/56266.pdf (Accessed 17 August 2015).
[57] Ueckerdt F, Hirth L, Luderer G, Edenhofer O. System LCOE: What are the costs of variable renewable? Energy 2013;63:61–75.
[58] Vestas. Offshore V164–8.0MW V112-3.3MW (tech. rep.). Aarhus, Dinamarca: Vestas Wind Systems; 2013. p. 15. Available, http://pdf.archiexpo.com/pdf/vestas/offshore-v164-80-mw-r-v112-33-mw/88087-243525.html [Accessed 07 September 2015].
[59] Villarrubia M. Energía Eólica. Primera edición. Barcelona, España: Ediciones CEAC; 2004. p. 328.
[60] Watts D, Jara D. Statistical analysis of wind energy in Chile. Renew Energy

2011;36:1603–13.
[61] Weisser D. A wind energy analysis of Grenada: an estimation using the 'Weibull' density function. Renew Energy 2003;28:1803–12.
[62] Wieringa J. Representative roughness parameters for homogeneous terrain. Boundary-Layer. Meteorology 1993;63:323–63.
[63] Zolezzi JM, Garay A, Reveco M. Large scale hydrogen production from wind energy in the Magallanes area for consumption in the central zone of Chile. J Power Sources 2010;195(24):8236–43.

Nomenclature

V: Magnitude of the wind speed at 10 m
$\vec{u}$: Wind component u (East-West)
$\vec{v}$: Wind component v (North-South)
V_z : Estimated wind speed at height Z_Z (m/s)
V_i : Wind speed at height for which data are available (m/s)
Z_Z: Height at which the speed is being evaluated (m)
Z_0: Surface roughness length (m)
Z_i: Height for which data are available (m)
$p(V_z)$: Wind probability density
α: Scale parameter
β: Shape parameter
A: Slope of lineal regression
B: Intercept of lineal regression
P/A_b: Wind energy potential
P: Wind energy (W)
A_b: Swept area (m2)
ρ: Air density (Kg/m3)
E: Wind energy produced
$P(V_z)$: power of wind turbine at a determined speed (wind turbine curve)
T: time period under study (hours)
CF: Capacity factor
PE: Estimated output
PN: Rated output
ηEST : Wind turbine's seasonal performance
E_d: Available wind energy
$\langle P \rangle$: Functioning turbine's annual average power output
$\langle P_d \rangle$: Average annual wind energy power available
$LCOE$: Levelized Cost of Energy
I_t: Investments at time t
M_t: Maintenance and operating costs at time t
E_t: Energy generated at time t
r: Discount rate of the evaluation
t: Time from zero up to the number of years the project lasts
NPV: Net Present Value
FC_t: Cash flow for a specific time period
IRR: Internal Rate of Return
PB: Pay-Back